Energy gaps of the two-dimensional electron gas explored with equilibrium tunneling spectroscopy

R. C. Ashoori,* J. A. Lebens,† N. P. Bigelow,‡ and R. H. Silsbee
Laboratory of Atomic and Solid State Physics, Cornell University, Ithaca, New York 14853
(Received 14 October 1992)

We detail our results revealing a new energy gap present in the two-dimensional electron gas (2DEG). The gap, seen in the tunneling spectrum of electrons in the 2DEG, develops only in the presence of a magnetic field applied perpendicular to the 2DEG plane. The experiments discussed here consist of measurements of electron tunneling between a 2DEG in a quantum well and an n^+ substrate using excitation voltages less than k_BT/e. At low temperatures and only with the magnetic field applied perpendicular to the plane of the electron gas in the well, the tunneling rate develops an unusual temperature-dependent suppression. The suppression strength is roughly independent of Landau-level filling for densities 0.5×10^{11} cm^{-2} to 6×10^{11} cm^{-2}. At low temperatures the application of an additional ac excitation voltage, with amplitude larger than k_BT, increases the tunneling conductivity. Using large enough excitation, the tunneling conductivity returns to its high-temperature value. This behavior suggests the existence of a magnetic-field-induced energy gap, at the Fermi level, in the tunneling spectrum of electrons in the 2DEG. The 2DEG density can be tuned continuously in our samples. Oscillations are seen in the tunneling conductivity as the 2DEG density is varied, consistent with Landau-level structure observed in magnetocapacitance measurements on the same sample. While the amplitude of the magnetocapacitance structure is a strong function of temperature through the temperature range down to below 1 K, strikingly, contrast in the oscillations in the tunneling rate ceases to develop as the sample temperature is decreased below the width of the gap. In other words, the presence of the gap appears to blur density-of-states features of energy width smaller than the gap width. At zero magnetic field no temperature dependence of the tunneling is observed except at 2DEG densities below 0.5×10^{11} cm^{-2}. At these low densities, the tunneling conductivity is also suppressed as the temperature is lowered. We believe that this suppression arises due to an energy gap caused by localization effects. For the lowest densities, this gap is likely a manifestation of the Coulomb gap. Interestingly, both the magnetic-field-induced energy gap and the gap observed at low densities lead to similar temperature dependencies of the tunneling conductivity.

I. INTRODUCTION

The two-dimensional electron gas (2DEG) in semiconductors has been studied in great detail using a number of experimental probes. The work presented here is unique in that it probes the tunneling density of states (DOS) around the Fermi energy of the 2DEG in the presence of a quantizing magnetic field. Until recently, the technique presented here and described briefly in Ref. 1 was the only method for studying zero bias tunneling from the 2DEG in semiconductors. In the last two years, two techniques which allow independent contact to a 2DEG in the proximity of a tunnel barrier have been developed by Smoliner *et al.*[2] and Eisenstein *et al.*[3] The results presented in this paper grew from a study intended to probe the modification of the density of states in the 2D electron gas produced by a magnetic field perpendicular to the plane of the gas, a measurement of "the Landau-level DOS at the Fermi level." The technique used provided two independent measures of the DOS, one a Landau-level DOS determined using magnetocapacitance measurements and explored elsewhere,[4,5] the other a tunneling DOS described here. The experiment extends earlier capacitance spectroscopy of the Landau-level DOS (Ref. 6) to lower temperatures and, most importantly, also measures the tunneling conductivity between the 2D gas and an n^+ substrate.

It differs as well from other tunneling measurements[7,8] which determine an I-V characteristic. In our experiment, the Fermi energy in a quantum well is varied in a controlled fashion by application of a gate voltage, and the Fermi energies on both sides of the tunnel barrier are kept within k_BT of one another. We measure the equilibrium tunneling conductivity as a function of the Fermi energy in the well, not the more usual differential conductivity as a function of the difference in Fermi energies across the barrier.

The experiment shows, in addition to the structure expected from the development of Landau levels, an unexpected suppression of the electron tunneling which is greater than an order of magnitude at a field of 8 T and a temperature of 100 mK. We interpret these data as evidence for the development of a new magnetic-field-induced energy gap forming at the Fermi energy of the 2D gas.[1]

This paper is divided into two parts. First we explore the temperature dependence of tunneling data taken in the presence of magnetic field perpendicular to the plane of the 2D electron gas. We then turn to data taken in the absence of magnetic field. Unlike the data taken in the presence of magnetic field, these data show no temperature dependence except at low electronic densities in the well ($<5\times10^{10}$ cm^{-2}), where the data again reveal a tunneling suppression as the temperature is lowered. Strangely, the two different tunneling suppression effects have similar temperature dependencies. This similarity

0163-1829/93/48(7)/4616(13)/$06.00

may indicate that related physical mechanisms are responsible for the tunneling suppression in the two cases. At the tend of the paper, we offer a possible explanation for the suppression effects seen at low density as well as speculations regarding the suppression effects induced by a magnetic field.

II. SAMPLES AND METHOD

Mesas etched from three wafers grown using molecular beam epitaxy have been studied. The essential structure of the wafers is shown in Fig. 1(a). The three wafers, **A**, **B**, and **C**, are described in Table I and in further detail elsewhere.[5] Also, tunneling measurements on sample **A** have been described in previous publications.[1,9–11] Each wafer consists of a degenerately n-doped substrate in GaAs, an $Al_xGa_{1-x}As$ tunnel barrier, a GaAs quantum well, a thick nonconducting (blocking) $Al_xGa_{1-x}As$ barrier which in wafers **A** and **C** contains an n-doped layer, and a degenerately doped GaAs surface contact region. In all wafers, only the lowest electronic subband of the well is occupied. The electron density in the quantum well can be varied by the application of a gate bias across the sample. The data presented in this paper concentrate mostly on the results from sample **A**; over 200 000 capacitance measurements were taken on one 400-μm-diam mesa produced on this wafer.

The geometry of our samples precludes us from directly measuring the 2DEG mobility. However, elastic scattering times in the well can be estimated in the three wafers from the widths of the DOS peaks of Landau levels in a magnetic field.[12] Elsewhere,[4,5] we have measured the Landau-level DOS using magnetocapacitance measurements. Because the Landau-level DOS peaks fit well to Lorentzian line shapes, we can estimate elastic scattering times, and hence nominal sample mobilities from the half-width Γ of the Lorentzian line shapes, $\tau_s=\hbar/\Gamma$. This formula gives a nominal 2.0-K mobility of approximately 21 0000, 25 000, and 15 000 $cm^2 V^{-1} sec^{-1}$ for the wafers **A**, **B**, and **C**, respectively. Actual transport mobilities are expected to be substantially higher (i.e., factor of 10).[13] Evidence for a magnetic-field-induced energy gap in the 2DEG has been observed in all three samples.

Tunnel barriers in our samples can be regarded as capacitors shunted by a tunneling conductance. These were designed to have RC times which lie within the range of our measurements. The capacitance and the loss tangent of patterned mesas were measured at 20 frequencies between 15 Hz and 30 kHz. Low-pass filtering[5] was employed on sample leads to reduce any noise that might cause spurious voltage excitation across the tunnel barrier. The loss tangent displays a Debye line shape which peaks, and concurrently the measured capacitance decreases, as the measuring frequency is swept through $1/2\pi RC$. The behaviors of the capacitance and the loss tangent in sample **B** as a function of frequency are shown in Fig. 2. We name low- and high-frequency limiting capacitances C_{low} and C_{high}, respectively.

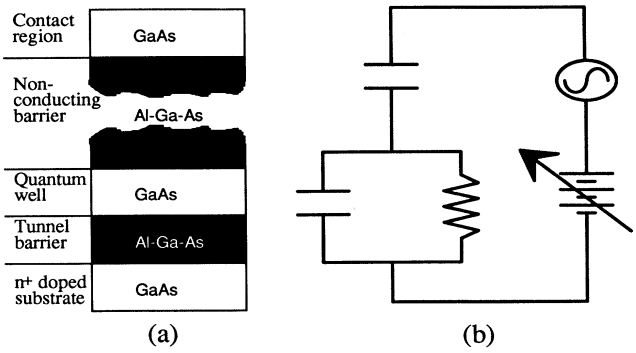

FIG. 1. (a) shows the essential structure of the samples. Tunneling from the GaAs quantum well to the substrate across the AlGaAs tunnel barrier is observed by means of capacitive coupling through the thick nonconducting barrier. (b) displays a simplified model of the sample.

Figure 1(b) shows the model which we use to characterize our set of capacitance and loss tangent versus frequency data. The data can be fit with suitable choices for the three circuit elements shown. If the thermodynamic DOS,[14–16] $\partial n/\partial\mu$ (see Appendix), in the well were infinite, the value of the conductance (resistor shown in the figure) obtained by these fits would be the tunneling conductance. With a finite DOS, this correspondence no longer holds; the capacitances shown in the model depend both on sample dimensions and the thermodynamic DOS in the quantum well.[4,5]

The Appendix of this paper presents an analysis of charge equilibration in our devices. This work yields the frequency-dependent impedance of our samples in terms of the tunneling rate of electrons from the substrate to the quantum well. The sample capacitance as a function of frequency takes the form

$$C(f)=\frac{C_{high}C_{low}[1+(f/f_{peak})^2]}{C_{high}+C_{low}(f/f_{peak})^2}\ , \tag{1}$$

where f_{peak} is the frequency at which the loss tangent achieves a peak. The tunneling conductance can be ex-

TABLE I. Growth parameters for the samples.

Sample	GaAs spacer layer (Å)	Tunnel barrier (Å)	Blocking barrier (Å)	Si dopants (from well edge) (Å)	Dopant concentration (cm^{-3})
A	30	160	1550	100–200	5×10^{17}
B	30	133	800	no dopants	no dopants
C	150	150	800	150–500	6×10^{17}

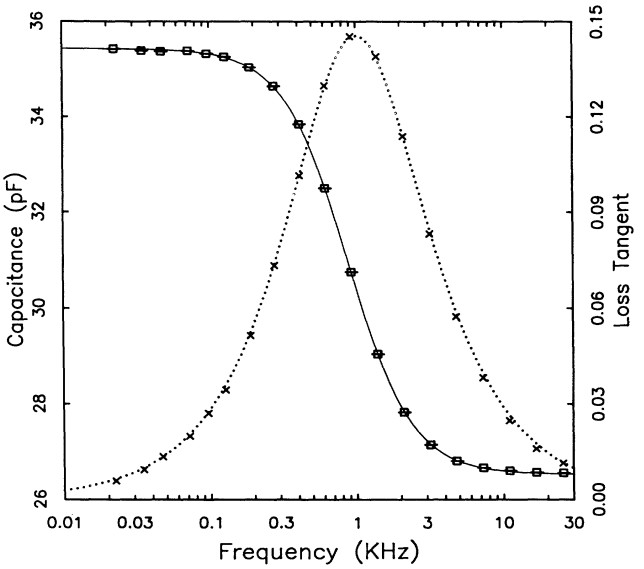

FIG. 2. Capacitance (squares) and loss tangent (crosses) of a 200-μm mesa etched on sample B. The solid and dotted curves are fits from the circuit model presented in Fig. 1(b). At low frequencies, electron transfer from the substrate to the well can take place, and the capacitance C_{low} is measured. At frequencies high compared to the inverse RC time of the tunnel barrier, no electron transfer to the well takes place, and the measured capacitance C_{high} drops to a value consistent with the distance from the top gate to the substrate layer.

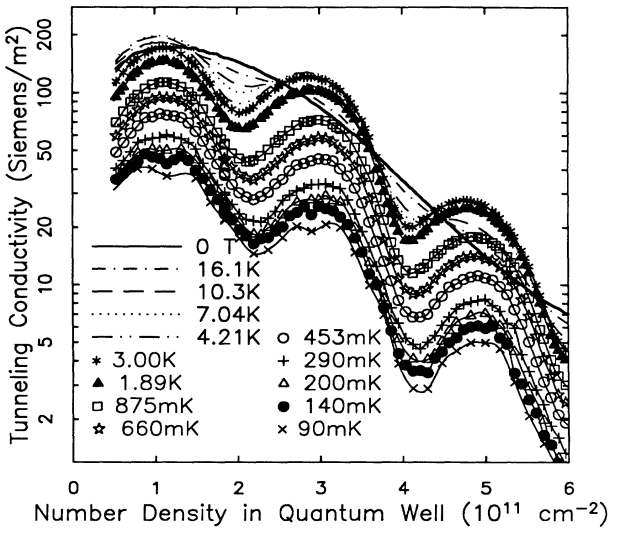

FIG. 3. Tunneling conductivity in sample A (log scale) vs electron number density in the quantum well for zero field (bold solid curve) and for a variety of temperatures with 4.0-T magnetic field applied perpendicular to the plane of the electron gas in the quantum well. The minima at densities of 2×10^{11} and 4×10^{11} cm^{-2} correspond to Landau-level indices of $\nu=2$ and $\nu=4$, respectively. The smooth curves joining the points are guides to the eye.

tracted from the three fitting parameters C_{low}, C_{high}, and f_{peak} using the relation

$$G_{\text{tun}}=2\pi f_{\text{peak}}C_{\text{geom}}\frac{C_{\text{geom}}}{\sqrt{C_{\text{low}}C_{\text{high}}}}\left[\frac{C_{\text{low}}}{C_{\text{high}}}-1\right]. \quad (2)$$

C_{geom}, described elsewhere,[4,5] is the "geometric" capacitance between the 2DEG and the substrate 3DEG (i.e., the capacitance between these two layers if the density of states in the 2DEG were infinite). The value of C_{geom} used here is extracted from other measurements and is known to within 2%.[4,5] We now discuss the results of a series of experiments in which the tunneling conductivity is measured in magnetic field applied perpendicular to the plane of the 2D electron gas as a function of the electron density in the quantum well, the temperature of the sample, and the magnetic-field strength.

III. TUNNELING IN THE PRESENCE OF MAGNETIC FIELD

Figure 3 displays the logarithm of the tunneling conductivity of sample A at 4 T for different temperatures. The highest-temperature curves oscillate about the zero field curve,[9] indicating the development of Landau-level structure in the DOS in the 2D gas. At lower temperatures, the tunneling conductivity is strongly suppressed. In contrast with this behavior in magnetic field, the zero field tunneling conductivity shows no substantial variation with temperature over the range 90 mK–10 K except for electron densities near full depletion ($<1\times10^{11}$ cm^{-2}). The temperature-dependent suppression occurs only in the presence of the magnetic field applied perpendicular to the plane of the 2D electron gas; a magnetic field applied parallel to the plane,[10] though changing the shape of the tunneling conductivity versus 2DEG density curve, does not induce a temperature-dependent suppression. We note that the doping levels in the substrate are high enough (10^{17} cm^{-3}) to discount magnetic freezeout[17] as the cause of the effect. Finally, the Landau-level DOS in the well, as determined from the capacitance values distinct from conductivity results, shows no unexpected behavior reflecting the tunneling suppression.

The temperature dependence suggests that the suppression is due to a tunneling anomaly restricted to energies near the Fermi energy. To explore this idea, a high-frequency signal (period shorter than the RC relaxation time of the tunnel barrier) was injected across the sample during capacitance measurements. This signal provides an oscillating Fermi-level offset between the 2D gas and the substrate, allowing tunneling to occur from a band of states of width given by double the amplitude of the injected signal. We find that as the excitation voltage that appears across the barrier due to the injected signal is made larger than k_BT/e, the suppression effects induced by the low temperature of the sample recede. At very low temperatures, where the suppression appears to be saturated, the effect of excitation, of rms amplitude V_e, on conductivity is roughly the same as increasing the temperature in absence of excitation to a value eV_e/k_B. This implies that the suppression would be observed in a conventional I-V characteristic as a zero bias anomaly, not as a general bias-independent suppression.

The data shown in Fig. 3 are striking in that the suppression depends in a substantial way neither on the electron density in the well over a concentration of $(0.5-6)\times10^{11}$ cm^{-2} nor on whether the Fermi level is at a maximum or minimum in the Landau-level DOS despite a ratio of the maximum to minimum DOS of about 10:1.[4,5]

In Fig. 3, tunneling at densities higher than 3.9×10^{11} cm^{-2} should be forbidden in the absence of scattering. At these densities, the Fermi level is in the third Landau level in the well, whereas in the substrate the third Landau level lies outside of the Fermi surface. Indeed, the tunneling conductivity is markedly lower in this range of density. Interestingly, the strength of suppression due to the magnetic field is approximately the same in the forbidden region as it is in the range of densities for which tunneling is allowed. This observation suggests that the suppression is not some consequence of the change in spatial character of the one-electron wave functions associated with the development of Landau states.

The data of Fig. 3 also display another interesting feature. As the sample is cooled from the highest temperatures, Landau-level structure begins to develop. Strangely, below around 7 K, the amplitude of the Landau-level oscillations ceases to develop further. In contrast, magnetocapacitance measurements show increasing amplitude of Landau-level structure down to temperatures below 1 K. Moreover, at low temperatures the ratio of the tunneling conductivity at a Landau maximum to that at a Landau minimum is about 2:1 while the Landau-level DOS measurements, as derived from capacitance results,[4,5] reveal a nearly 10:1 ratio below 1 K. It is suggestive that the amplitude growth of the conductance oscillations ceases at the same temperature at which the tunneling suppression effect commences.

For completeness, we show tunneling conductivity versus number density curves in the same sample for different magnetic-field strengths. Figure 4 displays the tunneling conductivity at various temperatures for a 2.0-T applied magnetic field. The tunneling suppression here appears to be weaker and sets in at lower temperatures than for the data in Fig. 3. For data taken at 8.5 T, shown in Fig. 5, strong suppression commences at higher temperatures than for the data of Fig. 3. In Fig. 5, the first two peaks that appear in the tunneling conductivity correspond to the spin split bands of the lowest Landau level. At 8.5 T, the second Landau level in the substrate is outside of the Fermi surface, and tunneling at electron densities above 4.1×10^{11} cm^{-2} should be forbidden. Once again, despite the sharp decrease in the tunneling conductivity as the electron density is increased into this forbidden region, the temperature-dependent tunneling suppression still persists.

Figure 6 displays the tunneling conductivity of sample **B** at 4 T and at 1.9 and 4.2 K. The same suppression effect occurs in this sample as in sample **A**. Notice that while there is some increased definition of the Landau level as the temperature is decreased, the suppression strength is again roughly independent of the 2D electron gas density. As with the data of sample **A**, on average the conductivity at 1.9 K is again about 20–30 % less than the conductivity at 4.2 K. We have data in sample **C** only at temperatures of 4 K and near 6 K. The suppression effect is observed in this sample as well although it is somewhat less apparent because, as with sample **A** in this temperature range at this magnetic-field strength, the strength of the suppression is small and there is at the same time considerable temperature dependence of the Landau-level widths.

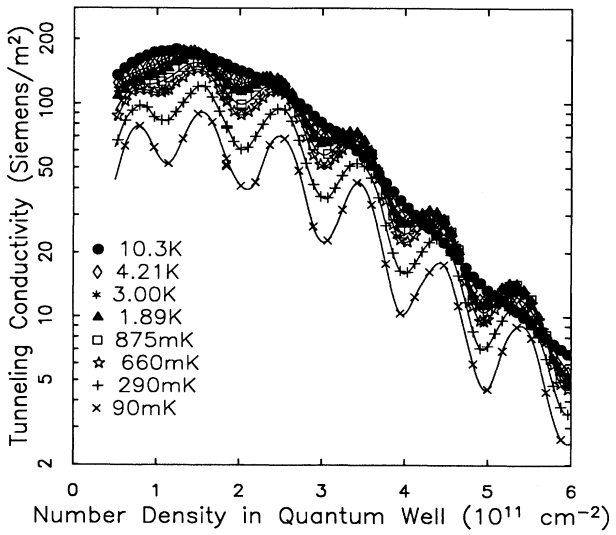

FIG. 4. Tunneling conductivity in sample **A** vs electron number density in the quantum well at 2-T magnetic field applied perpendicular to the plane of the electron gas in the quantum well. The oscillations here correspond to spin-degenerate Landau levels, the first peak shown being the lowest level.

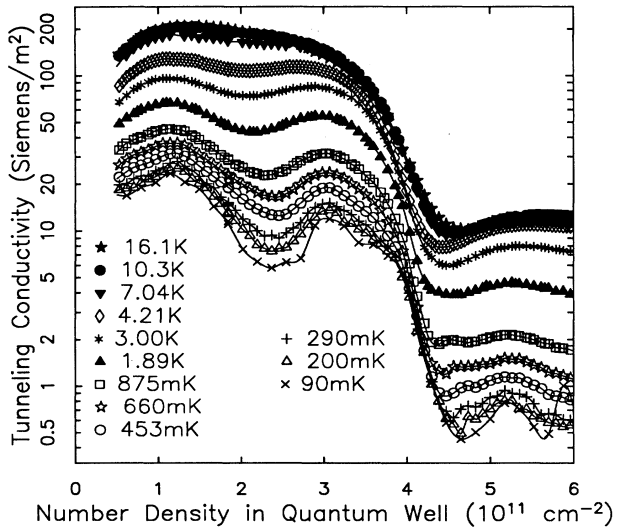

FIG. 5. Tunneling conductivity in sample **A** vs electron number density in the quantum well at 8.5-T magnetic field applied perpendicular to the plane of the electron gas in the quantum well. The first two peaks shown as the density is increased are the spin split levels of the lowest Landau level. Note that the vertical scale is different here than in Figs 3 and 4.

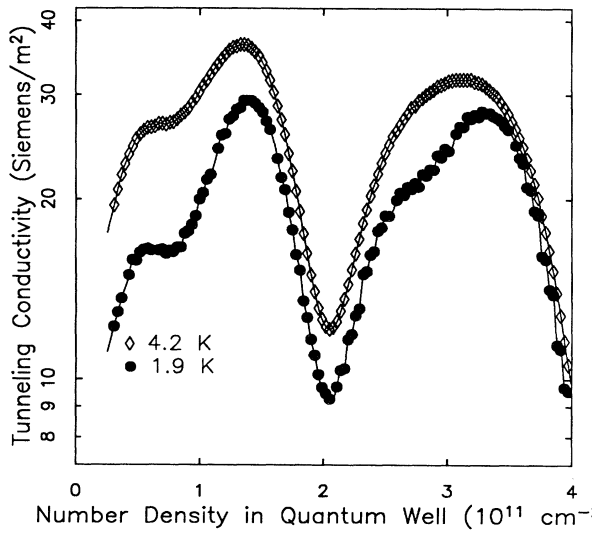

FIG. 6. Tunneling conductivity vs number density in sample **B** at a magnetic field of 4.0 T. The suppression effect is clearly visible in this sample. Also apparent is the spin splitting of the Landau levels which becomes increasingly prominent as the temperature is reduced. The minimum at density 2×10^{11} cm^{-2} corresponds to Landau-level index $\nu=2$.

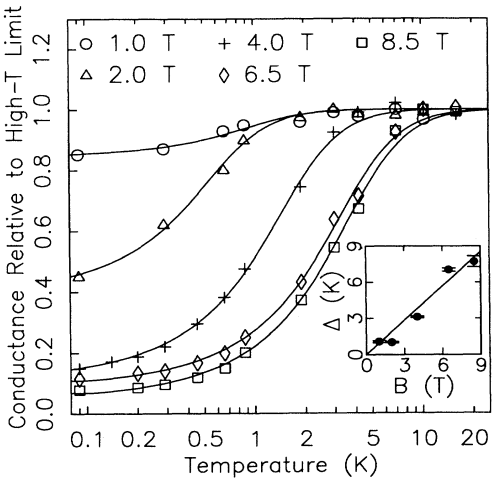

FIG. 7. Plotted as symbols are the averaged conductances relative to the high-temperature limit of the conductance plotted against temperature (log scale). The smooth curves are fits described in the text. Shown in the inset is Δ in kelvins plotted against the applied magnetic field. The line is given by $\Delta=0.047\hbar\omega_c/k_B$.

IV. AVERAGE CONDUCTIVITY

Figure 7 gives a global summary of our results from sample **A**. The data points give $\Lambda(T;B)$, the average of the ratio of the tunneling conductivity at temperature T and field B to the conductivity at temperature T in zero field. The averaging is over a range of energies corresponding to a filling of the well spanning a half integral or integral number of Landau levels. The averaging is needed to isolate changes in the tunneling conductivity arising from the tunneling suppression from changes in the conductivity due to varying detail in the Landau-level structure, such as increased contrast or the appearance of spin splittings, which develops at the lower temperatures.

There is a subtlety involved in determining the average value of the tunneling conductivity. The average of the conductivity must be taken with respect to the Fermi energy in the well, not with respect to the carrier density in the well, to assure that changes in contrast of the Landau-level structure, important only at the highest temperatures, do not contribute to an apparent but unreal change in the average of the tunneling conductivity. The conversion between well filling (nearly proportional to the gate voltage) and Fermi energy is accomplished using magnetocapacitance data.[4,5]

We choose to characterize our results in terms of a "tunneling density of states" $g_s(E;B)$ which reflects the effects of the magnetic-field suppression and a tunneling rate $1/\tau_{\rm tun}(E)$ which is assumed uninfluenced by the magnetic field and to vary with energy slowly on the scale of k_BT. At zero temperature, the tunneling conductivity of the sample would be

$$G(T=0;B;E_F)=e^2\frac{g_s(E_F;B)}{\tau_{\rm tun}} . \quad (3)$$

At finite temperature, the $g_s(E;B)$ in Eq. (3) should be replaced by a suitable thermal average[18] to give, for the conductivity,

$$G(T;B;E_F)=-\frac{e^2}{\tau_{\rm tun}(E_F)}\int_0^\infty g_s(E;B)\frac{\partial f(E;T)}{\partial E}dE , \quad (4)$$

where $f(E;T)$ is the Fermi distribution function, E is the kinetic energy of electrons in the 2D electron gas, and E_F is the Fermi energy in the well measured with respect to the bound-state energy in the well.

The data points in Fig. 7, in this framework, correspond to the experimental values represented by

$$\Lambda(T;B)=-\int_0^\infty\frac{g_s(E;B)}{g_0(E)}\frac{\partial f(E;T)}{\partial E}dE , \quad (5)$$

where $g_0(E)$ denotes the tunneling DOS in the absence of magnetic field. For all but the 8.5-T data, $\Lambda(T;B)$ at high temperatures approaches a well-defined value of one which is taken to be the high-temperature limit. Ambiguities of interpretation at high temperature imply a 10% uncertainty in the normalization of the 8.5-T data.

For interpretation of the results we model the data with $g_s(E;B)$, containing a gap, of the form

$$g_s(E;B)=Sg_0+\frac{(1-S)g_0|E-E_f|}{\Delta}\quad(E\le2\Delta) ,$$
$$g_s(E;B)=g_0\quad(E>2\Delta) , \quad (6)$$

with $g_0(E)=g_0$, independent of E. The smooth curves of Fig. 7 are generated from Eq. (5) using this "linear" gap with a tunneling density of states S at the Fermi energy and width Δ depending on B.

We call attention to a few principal features of the summary data in Fig. 7 and of the fits. (a) For low fields,

1 and 2 T, the width parameter Δ depend little on B, but the depth of the gap $(1-S)$ increases with increasing field. (b) For high fields, 6.5 and 8.5 T, the gap is nearly fully developed in depth and the width is increasing with field, with some indication of saturation at high fields. (c) The data at 4 T and below consistently show more temperature dependence in the low-temperature limit than do models in which the gap is nonsingular at the Fermi energy, e.g., square or smooth bottomed gap functions. At the fields of 6.5 and 8.5 T, the data deviate from the fits at low temperatures, displaying a weaker temperature dependence than would be suggested by the linear gap model. This may indicate a "flattening" of the gap's minimum (hardening of the gap) as it saturates in depth. (d) At fields 2 T and higher, the gap width Δ has a value of about 5% of the cyclotron energy, $\hbar\omega_c$ (see inset to Fig. 7).

We interpret the results in terms of a gap, rather than of an influence of the field on the single-particle tunneling dynamics, because the temperature and excitation dependencies indicate that the tunneling is suppressed only for states near the Fermi energy. Before discussing possible candidates for such a gap, or other proposals, we turn first to another tunneling suppression that we have observed.

V. LOW-DENSITY TUNNELING SUPPRESSION IN THE ABSENCE OF MAGNETIC FIELD

As noted above, in the case of zero magnetic field or magnetic field parallel to the plane of the 2D electron gas, no temperature-dependent tunneling suppression is observed for most of the range of densities of the 2D electron gas. However, temperature dependence *is* observed at densities below $\approx 0.5\times10^{11}$ cm^{-2}. Figure 8 displays the tunneling conductivity (obtained in a model described in the next section) in sample **A** as a function of device gate bias for sample temperatures ranging from 95 mK to 16 K. The shape of this curve at densities above 1.2×10^{11} cm^{-2} has been explained previously in terms of momentum conservation rules in tunneling.[9,11] For gate voltages above about -800 mV (about 1×10^{11} cm^{-2} mean well density as determined from magnetic-field measurements), low-frequency capacitance measurements indicate that the quantum-well area is fully occupied. At voltages below -800 mV a significant temperature dependence of the conductivity appears. As in the case of perpendicular applied magnetic field, the tunneling conductivity is suppressed as the temperature is decreased. Similar suppression at low densities has been observed as well in samples **B** and **C**. The technique used to plot the tunneling conductivity here differs at low densities from that used in previous figures. The next few paragraphs describe the differences as well as why a different method is needed in the low-density limit.

A. Capacitance versus frequency curve fitting in the low-density regime

Equation (2) above yielded the tunneling conductivity of samples in terms of the loss peak frequency and the low- and high-frequency capacitances of the device. This relation, as well as the framework used in developing it,

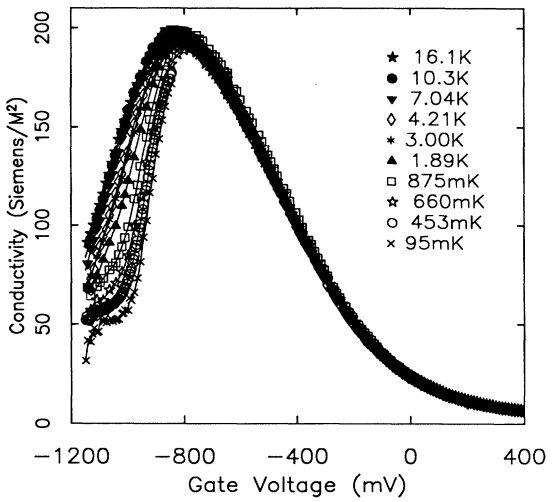

FIG. 8. Tunneling conductivities (linear scale) in zero magnetic field vs gate voltage in sample **A** at temperatures ranging from 95 mK to 16.1 K. Note that at a gate voltage of -800 mV, the electron density is about 1×10^{11} cm^{-2} and rises linearly with gate voltage to a value of around 6×10^{11} cm^{-2} at a gate bias of 400 mV. Below -800-mV gate bias, the quantum well begins to depopulate nonuniformly, leaving unoccupied regions of the well. In this region, the electron density is no longer linear in gate bias, and the rate of electron density change with gate bias is decreased. The conductance is obtained from the capacitance data using the "puddling" model described in the text.

breaks down at low electron densities in the well if there are portions of the well unoccupied by electrons. Experimentally, a decrease in the low-frequency capacitance of the device is observed as the gate bias is lowered in the low-density region. We explore here reasons for this decrease and develop interpretations of the capacitance and loss data in the low-density regime.

We proceed to model the sample with low densities in the well using the assumption that occupied and unoccupied regions of the sample are larger than a few hundred angstroms in size so that fringing fields can be neglected. Because there are unoccupied regions of the well, a capacitance shunting the top gate to the substrate must be added to the circuit model of Fig. 1(a). We note that, in the absence of electrons in the quantum well, the sample capacitance is equal to $C_{\rm high}$. The shunting capacitance in the model then has a value of $C_{\rm high}(1-\alpha)$ where α is the fractional area of the 2D electron gas which is occupied by electrons. This sample model is shown in the inset of Fig. 9. The division of the device this way into two regions, one depleted and the other filled with electrons, gives the form

$$C(f)=\frac{\alpha C_{\rm high}C_x[1+(f/f_{\rm peak})^2]}{C_{\rm high}+C_x(f/f_{\rm peak})^2}+(1-\alpha)C_{\rm high} \qquad (7)$$

for fits to capacitance versus frequency curves. The parameter C_x is the capacitance that *would* be measured at low frequencies if the well were fully occupied. The measured low-frequency capacitance $C_{\rm low}$ is given by

$$C_{\rm low}=\alpha C_x+(1-\alpha)C_{\rm high}\ .$$

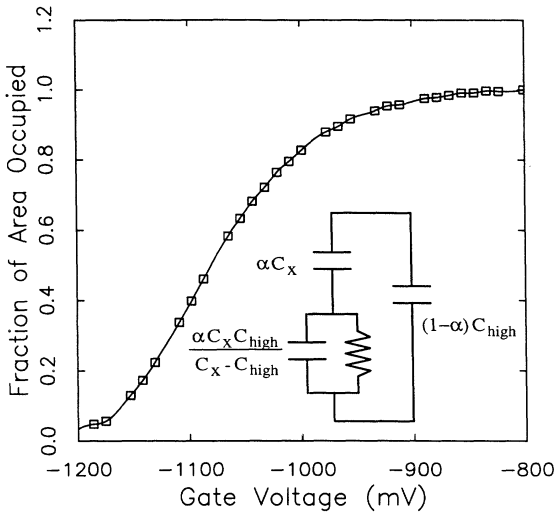

FIG. 9. Displayed is the fractional areal occupation of the quantum well, α, as determined from capacitance vs frequency curves fitted by Eq. (7) and the model of Fig. 14. The solid curve is a guide to the eye. Inset: The circuit model used to fit capacitance vs frequency curves taken in the low-density region of the device operation. The capacitance on the right, $(1-\alpha)C_{\text{high}}$, is the capacitance measured from unoccupied regions of the quantum well. The two capacitor model on the left corresponds to the regions in the quantum well which are occupied by electrons.

At this point, fits can be made to the capacitance data using C_{low}, C_{high}, α, and f_{peak} as fitting parameters.

Attempts to make such fits show the experimental accuracy inadequate to define independently values of α and of C_x. Instead we consider two limiting cases of the model. In the first we set $\alpha=1$; the model considers the system to be a uniform 2DEG and all changes in device capacitance are attributed to variations in the DOS in the well which will be reflected in variations of the fitting parameter C_x. We call this the "filled well" model.

In the second case, the "puddling" model, we use Eq. (7) and fix the value of C_x as follows. We observe that for gate biases corresponding to the well surely full, the ratio $C_{\text{low}}/C_{\text{high}}$ is very nearly independent of gate bias (in the absence of magnetic field). We take that value to represent the ratio C_x/C_{high} for the filled areas (puddles) of the well by assigning the value $(C_x/C_{\text{high}})_{\text{puddles}} = (C_{\text{low}}/C_{\text{high}})_{\text{full well}}$ determined from data with full occupation of the well.

We have chosen to use the puddling model for several reasons. (a) Using the filled well model leads to conductivity versus gate bias curves in which the tunneling conductivity falls very rapidly at low densities, much faster than does the device capacitance at low densities. This is in strong contradiction with the simplest model in which the conductivity depends only on the DOS in the well, and would require major modification by interaction effects. (b) Data analysis leaving both α and C_x as free parameters, though ambiguous, favors the puddling model. (c) The puddling model is a commonly used model[19] for treating heterojunctions near full depletion.

We restrict our attention now to the puddling model with the caveat that, in reality, we expect a decrease in conductivity at low density both because of band tailing (the filled well model) and because of full depletion of some areas of the sample (the puddling model).

The tunneling conductance is easily evaluated in the puddling model as

$$G_{\text{tun}} = 2\pi f_{\text{peak}} \alpha C_{\text{geom}} \frac{C_{\text{geom}}}{\sqrt{C_x C_{\text{high}}}} \left[\frac{C_x}{C_{\text{high}}} - 1 \right] . \tag{8}$$

Of course, what is interesting physically is not the total conductance, but the conductance per unit filled area, which is this formula divided by the quantity αA, where A again is the area of the mesa.

B. Detailed observation of low-density tunneling conductance

We use the puddling model framework to plot in Fig. 9, α, the fraction of the area of the quantum well which is occupied as a function of gate bias. The curve was obtained from data taken in zero magnetic field and at 1.85 K. We have fitted data of capacitance versus frequency from a variety of temperatures from 95 mK to 16 K and see little change in this curve. Within the resolution of these results, we observe no thermal smearing of the α versus bias curves up to the highest temperatures. In the following discussion we treat the occupied area and electron density as fixed at a particular gate bias, independent of sample temperature.

Figure 10 "zooms in" on the tunneling conductivity, determined in the puddling model, in the low-density region of sample **A** as a function of gate bias for tempera-

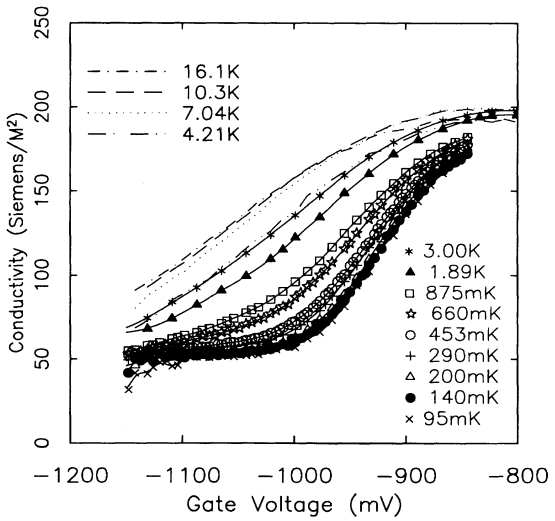

FIG. 10. The figure displays in detail the tunneling conductivity (conductance per unit occupied area) determined using Eqs. (7) and (8) for a variety of temperatures between 95 mK and 16.1 K. Two features of the plot stand out. First, there appear to be low- and high-temperature limiting values to the conductivity. The transition between these two values always occurs at between 0.5 and 3 K, independent of gate bias. Secondly, an unexplained plateau develops at low temperatures in the conductivity at biases below −1050 mV.

tures from 95 mK to 16 K. The temperature dependence is immediately striking. For the whole region of gate biases plotted, above around 7 K the conductivity saturates to a high-temperature limiting value; below about 500 mK the tunneling conductivity saturates to a low-temperature value. For the entire curve, most of the shift of the conductivity with temperature happens between 1 and 3 K. Another striking feature in Fig. 10 is the plateau which develops in the conductivity at low temperatures. The reason for this plateau, as well as the rest of the shape of the tunneling conductivity plot as a function of gate bias, is not understood.

C. Low-density conductivity as a function of temperature

At this point, we note the similarity of the temperature dependence of the tunneling conductivity at low densities to the tunneling suppression induced by a magnetic field illustrated in Fig. 7. In the case of the low-density data, we simply take the conductivity at a particular value of gate bias and plot it as a function of temperature. Figure 11 displays the conductivity relative to its high-temperature value plotted as a function of temperature for a gate bias fixed at -1050 mV. The resemblance of the shape of this curve to the curves of Fig. 7 is readily apparent. The solid line is a fit to the data obtained using Eqs. (5) and (6), the *same* gap function used to fit the magnetic-field data. In Fig. 11, Δ has a value of about 4.7 K, and the gap depth parameter S has a value of 0.4. By adjusting the values of Δ (which undergoes only slight variations with gate bias in the low-density regime) and S the gap model of Eq. (6) can be made to fit the data well for all but the lowest gate biases in the low-density region. We will return below to this similarity in the temperature dependencies of the two suppression effects.

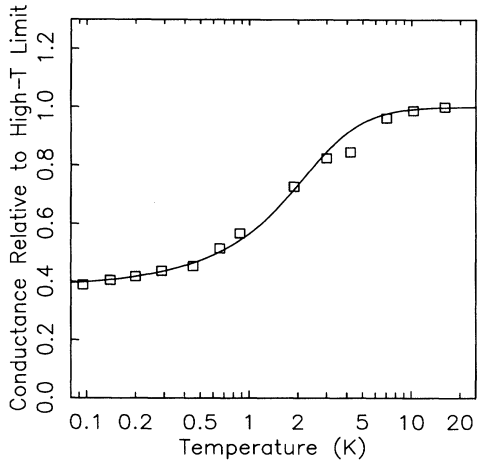

FIG. 11. Plotted as boxes is the conductivity from Fig. 10 at -1050 mV plotted as a function of temperature (log scale). The solid curve is a fit using Eq. (5) and the same "linear gap" of Eq. (6) that was used to fit the magnetic-field-induced suppression. The fit has Δ adjusted to a value of 4.7 K.

VI. LOW-DENSITY REGION WITH MAGNETIC FIELD APPLIED

Now that we have examined in detail both the suppression of tunneling by magnetic field at high densities and the suppression at low densities in zero magnetic field, it is interesting to ask, what happens at low density in the presence of a magnetic field? We again use the puddling model of the preceding section to fit the capacitance data and extract the tunneling conductivity.

Figure 12 displays the conductivity of sample **A** at a temperature of 290 mK at magnetic fields ranging from 0 to 8.5 T. At the highest fields, the magnetic-field conductivity suppression is still very strong at these low electron gas densities, and the 6.5- and 8.5-T curves remain well below the 0-T curve over the full range of gate biases shown. The data from lower fields show an intriguing behavior. At higher gate bias values in Fig. 12, the 1- and 2-T curves fall below the zero field curve due to the magnetic-field suppression. As the gate bias (and thus the average electronic density) is reduced, the low field curves merge at a certain gate bias with the zero field curve and then follow along the zero field curve as the gate bias is reduced further. This same behavior persists at a variety of different temperatures. Further, the curve at 2 T always merges with the zero field curve at gate biases between -950 and -975 mV, independently of the temperature.

The magnetic-field conductivity suppression at low densities has an electronic density dependence, unlike the suppression effect at higher densities. This density dependence provides a strong indication that the source of the field-induced conductivity suppression lies in the 2D electron gas and not in the substrate. Further, the merging behavior of the curves in Fig. 12 is suggestive

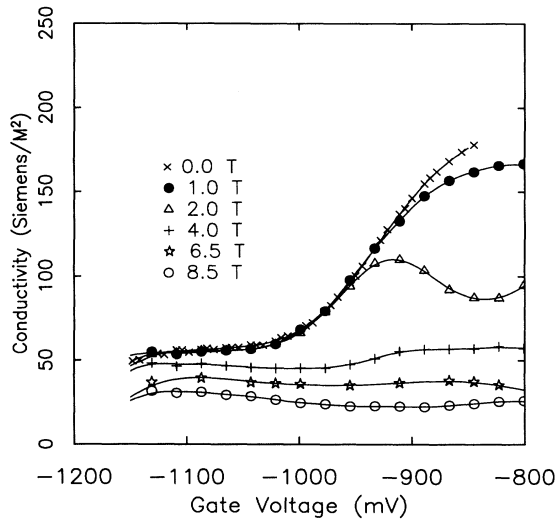

FIG. 12. Tunneling conductivity as a function of gate bias for different magnetic-field values at 290 mK. Notice that the curves taken at higher magnetic fields are significantly suppressed below the curve at zero field. Curves taken at 1 and 2 T display an interesting merging with the curve taken in absence of field as the gate bias is reduced.

that three regimes exist, a high-density regime where the magnetic-field suppression dominates, a low-density regime where the low-density suppression dominates and a crossover regime which is where the curves merge together.

VII. SPECULATIONS REGARDING POSSIBLE CAUSES FOR THE SUPPRESSION EFFECTS

We briefly review the main characteristics of suppression effects in the tunneling conductivity described above. A magnetic field, only when perpendicular to the plane of the 2D electron gas, produces a tunneling suppression that can be characterized by an energy gap at the Fermi energy in the 2D electron gas. We focus on the 2D electron gas as the source of the suppression for two reasons. First, anomalies in the 3D gas should be present for arbitrary orientation of the magnetic field, but the suppression is observed only with the field perpendicular to the 2D gas. Second, density dependence of the suppression is observed near depletion of the 2D gas, as described in the preceding section, suggesting the properties of the 2D gas as the source of the suppression effect. In the case of zero applied magnetic field, tunneling suppression is again observed at low densities of the 2D electron gas and can be characterized by the same "linear gap" that fit the data well in the case of the magnetic-field conductivity suppression in low magnetic fields.

A. Tunneling conductivity suppression at low densities

We first focus on the low-density zero field suppression because this low-density region of the 2D electron gas has shown a number of interesting properties previously, some of which are understood theoretically. Far-infrared absorption experiments[20] on the 2D electron gas in silicon metal-oxide-semiconductor field-effect transistors (MOSFET's) at low densities ($<4\times10^{11}$ cm^{-2}) have shown a frequency dependence of the electronic conductivity at photon energies below ≈0.5 mV. These have been explained by arguments invoking localization in a disordered system.[21] Also, in low-density inversion layers in silicon MOSFET's, Bishop, Tsui, and Dynes[22] have observed a logarithmic temperature dependence in the low temperature in plane conductivity of the 2D electron gas which they interpret in terms of localization models.

Altshuler, Aronov, and Lee[23] have suggested that localization effects should cause an energy gap to form at the Fermi energy in the tunneling DOS in disordered systems. In the simplest heuristic model, this gap arises for the following reasons. In a disordered material with a background random potential, electrons eventually find a configuration in which they minimize both their energy with respect to the random potential and also the energy associated with the electron-electron repulsion. Suddenly adding or subtracting another electron forces the system to rearrange and requires it to overcome energy hurdles to find a new stable state. In two dimensions, Altshuler, Aronov, and Lee predict that near the Fermi energy, this gap should have the form

$$\frac{\delta g(E)}{g(E)} = -\frac{\hbar}{2\pi E_F \tau_s} \ln\left[\frac{(E-E_F)\tau_s}{\hbar}\right] . \quad (9)$$

Tunneling experiments have been done in both thin indium oxide films[24] and in thin tin films.[25] In both of these experiments, the thickness of the films were varied to test certain aspects of the theory. These measurements, in cases where the films were thin enough to be considered two dimensional, have shown the logarithmic behavior in the tunneling conductivity as a function of the voltage across the tunneling barrier (at voltages <20 mV) expected from the Altshuler-Aronov-Lee theory.

We note that the gap used in Fig. 11 is, like the Altshuler-Aronov-Lee gap, singular (the derivative is discontinuous) at the origin. Indeed, a singularity was necessary to account for the low-temperature behavior of the tunneling conductivity. We are tempted to propose that the Altshuler-Aronov-Lee gap is the source of the tunneling suppression at low densities in our samples. However, there is a feature of the data of Fig. 10 inconsistent with this model. The temperature of the step in the tunneling conductance is roughly independent of the electron density, always lying in the range of 1 and 3 K. This is in contrast with Eq. (9) which predicts that the gap should deepen and widen as the Fermi energy is decreased. Lastly, we note that as the gate bias is reduced, the system will at some bias move to the insulating side of the metal-insulator transition. In this case, electrons are fully localized, and it is more appropriate to speak of a Coulomb gap.[26]

B. Tunneling conductivity suppression by a magnetic field

At present, we have no clear understanding of the mechanism which produces the apparent energy gap in the tunneling DOS in a magnetic field. The simularities between the temperature dependence of the low-density suppression results in Fig. 11 and the magnetic-field results in Fig. 7 lead us to speculate that these two effects might be different incarnations of the same underlying physics. The main problem with interpreting the magnetic-field results this way, however, is that one would expect the strength of the gap to depend upon the Landau-level DOS and/or the overall density; the Landau-level DOS varies by more than a factor of 10 (at the highest fields used here) as the Fermi energy moves from the center of a Landau level to between Landau levels. Our magnetic-field results instead indicate that the strength of the gap is independent of the position of the Fermi energy within the Landau-level structure and is roughly independent of electron concentration from 0.5×10^{11} to 6×10^{11} cm^{-2}.

Aside from an energy gap, another proposal for the cause of the tunneling suppression in magnetic fields is the enhancement, by some mechanism involving the magnetic field, of the coupling of the tunneling transition to other excitations of the system, e.g., phonons or plasmons. The limiting value of the suppression at low temperatures would, as observed, decrease with increasing field as more tunneling oscillator strength is transferred from the elastic to the inelastic channels.

There is no obvious candidate for the coupled excitation which would need to have a characteristic energy of order 0.5 meV in order to explain, even crudely, the temperature dependence of the suppression.

A magnetic field applied perpendicular to a 2DEG obviously induces electron correlations which can cause dramatic results (e.g., the fractional quantum Hall effect). At very low Landau-level filling fractions, a sharp increase in the 2DEG transport resistivity has been attributed to solidification of the 2DEG.[27] Electronic correlations are the cause of the gap we observe at low densities in the absence of magnetic field. It seems likely that correlations are also responsible for the gap at higher fillings in the presence of magnetic field. It remains a puzzle that unlike the fractional quantum Hall effect and Wigner crystallization, the tunneling gap that we have characterized is independent of the Landau-level filling fraction.

Finally we mention a characteristic of the magnetic-field data which may relate to the cause of the tunneling suppression in magnetic field. The amplitude of the oscillations due to the Landau-level structure is much smaller in the tunneling conductivity than in the Landau-level DOS. This is true for all three samples. At present, we have no explanation for this effect. Qualitatively, it appears that the curves taken at lower magnetic-field values (such as at 2 T), at the lowest temperature (well below 1 K), do achieve nearly the same 2:1 peak-to-valley ratios that are seen in the Landau-level DOS measurement. At higher magnetic-field strengths the 2:1 peak-to-valley ratio is not surpassed in the tunneling conductivity even though the Landau-level DOS results have much larger ($\approx$10:1) peak-to-valley ratios.

We find it intriguing that Landau-level DOS and tunneling results show the same amount of contrast at high temperatures where the Landau-level structure is nearly washed out due to thermal broadening. As the temperature is decreased both the Landau-level DOS and the tunneling conductivity results develop contrast equally. However, at some temperature (at around 7 K for the data at 4 T shown in Fig. 3), the tunneling data cease to develop contrast (or develop it only slowly) while the Landau-level DOS continues to show more contrast as the temperature is reduced. Interestingly, this bifurcation takes place at temperature around $2\Delta/k_B$, where Δ is the gap parameter. We speculate that the development of the gap may wash out features in the tunneling DOS of energy width on order of the gap energy.

C. Comparison to a recent experiment

Very recently, Eisenstein, Pfeiffer, and West[28] have presented evidence from an experiment, in many ways complementary to our own, confirming our prior observation[1] of the presence of a field-induced energy gap. They have studied the tunneling between two 2DEG's in a double quantum-well structure in fields in the range of 8 to 14 T. The gap structure is observed in the same geometry, magnetic field perpendicular to the plane of the 2DEG, and is similar in magnitude to that discussed here and in Ref. 1. This and other similarities between the two observed gaps lead us to conclude that the effects seen in the experiment of Eisenstein, Pfeiffer, and West are a manifestation of the same physics which produces the gap seen in our measurements. This conclusion is at odds with the discussion of Eisenstein, Pfeiffer, and West, who suggest that different physics is involved. They offer two arguments in support of this position.

Their first argument concerns the shape of the gap. The Eisenstein-Pfeiffer-West experiment consists of a measurement of the tunneling current between two parallel 2DEG layers separated by a 175-Å-wide tunneling barrier. In the presence of magnetic field perpendicular to the 2DEG layers evidence for a gap is manifested by a sublinear I-V characteristic (V being the applied voltage difference the two wells.) Eisenstein, Pfeiffer, and West contrast their "broad energy gap" structure seen in I-V characteristics with the linear gap model which we have used. Two points must be recognized. First, an I-V characteristic should not be directly contrasted with a density-of-states model; rather the I-V characteristic in their experiment will be given by the fold of the densities of states in the two wells,

$$I(V)=\frac{-e}{\tau_{\text{tun}}}\int_0^{eV} g_s(E)g_s(E-eV)dE \ . \tag{10}$$

A linear gap, $g_s(E)\sim|E-E_F|$, will produce a *cubic* I-V characteristic. A V^3 characteristic, while not following the Eisenstein-Pfeiffer-West data precisely, gives a reasonable fit. Second, there are no data in the Eisenstein-Pfeiffer-West paper for fields below 8 T. As most of our work has focused on the gap at fields below 8 T, it is difficult to make detailed comparisons.

They comment as well on the absence of a thermally activated regime in our data. The data they present to illustrate the thermal activation are at 13 T, well above our highest measuring field of 8.5 T. The results certainly point to a "harder" gap at this field. However, we again note that the tunneling between two 2DEG's each containing a gap, contrasted with that in a system containing a single 2DEG, will naturally *appear* to arise from a "harder" gap. Without more detailed analysis of their lower field results, however, it is an untenable leap to conclude that the origins of the gap are fundamentally different in nature.

Eisenstein, Pfeiffer, and West remark "While we speculate that our high field results derive from a pure 2D system, it seems plausible that theirs depend critically on the interplay of disorder and interaction." The results discussed in this paper at low concentrations do indicate suppression effects related to disorder. These results also indicate clearly that the crossover from disorder-dominated suppression to field-dominated suppression, the "smooth connection" hypothesized by Eisenstein, Pfeiffer, and West, occurs at concentrations below 5×10^{10} cm^{-2}. Furthermore, though the 2DEG mobility is expected to be at least ten times higher[29] in our sample at a density of 6×10^{11} as compared with 1×10^{11} cm^{-2}, we observe ostensibly *no* dependence of the magnetic-field-induced tunneling suppression on density in this range. The fact that the tunneling suppression is not ob-

served to vary as a function of Landau-level filling fraction is another statement of this insensitivity to disorder. As the filling fraction is varied, the localization length of states at the Fermi energy varies tremendously. Thus the magnetic-field-induced gap does not appear to depend on the extent of electron localization over the very broad range of localization lengths present in a Landau level. Except at the lowest 2DEG carrier densities, disorder appears to have no relation to the gap structure that we observe.

Our current view is that the experiment of Eisenstein, Pfeiffer, and West represents both a confirmation and an important extension of our results to higher field. We note also the two important advantages of our technique: the ability to study the gap over a wide range of carrier concentrations and in regimes in which the in-plane conductivity of the 2DEG is very low.

VIII. SUMMARY

In summary, we observe two novel tunneling suppression effects in the tunneling of electrons between a 2D electron gas and a 3D substrate. We have completed a detailed study of the temperature dependence of these effects. One of these, a tunneling suppression that occurs only for low densities of the 2D electron gas, may be related to the energy gap seen previously in tunneling from thin metal film systems and though to arise from electron-electron interaction effects in the presence of disorder. The other tunneling suppression effect occurs over a wide range of densities of the 2D electron gas in the presence of a magnetic field perpendicular to the plane of the 2D electron gas. This suppression can be characterized by a field-induced gap in the tunneling DOS tied to the Fermi energy of width roughly 5% of $\hbar\omega_c$.

ACKNOWLEDGMENTS

This work was supported by the Semiconductor Research Corporation, Grant No. 90-SC-069, and by the National Science Foundation, Grant No. DMR-8616727. We thank S. Wright, M. Heiblum, L. Pfeiffer, and K. West, who provided the wafers for this work. We thank Professor D. M. Lee and D. Hawthorne for experimental advice and support. The use of the National Nanofabrication Facility and the facilities of the Materials Science Center at Cornell were essential to the realization of this project.

APPENDIX: EXTRACTION OF TUNNELING CONDUCTANCE FROM CAPACITANCE DATA

1. Equilibration of 2D and 3D charge densities

In this appendix we describe how fits to curves of capacitance and loss tangent versus frequency are used to determine the tunneling conductance between the 2DEG and the substrate. To understand this problem, we first need to describe how the electron densities in the well and the substrate, starting slightly out of equilibrium, transfer electrons between one another through tunneling to bring the two charge densities into equilibrium. Once the time constants for approaching equilibrium are known, it is a simple matter to determine how the overall divice impedance behaves as a function of frequency. The device operation is more complicated than is suggested by the circuit model of Fig. 1(b) due to the finite density of states in the quantum well. In fact, both the tunneling DOS, g_s, and the thermodynamic DOS, g_d, must be taken into account to correctly deduce the tunneling conductance from the capacitance data.

Figure 13 shows the situation when the "quasi-Fermi level" in the quantum well E_{Fw} is greater than the Fermi level in the substrate, E_{Fs}. We are interested in the quantity $E_{Fw}-E_{Fs}$, as it describes the degree to which the electron gases are out of equilibrium. E_{Fw} is determined by the sum of two components. One is the energy of the bound state in the well with respect to the conduction-band edge deep within the substrate. The other is the width of the band of filled 2D electronic states within the well which arises from the finite thermodynamic DOS in the well. As the electronic charge in the well changes both of these energies change. The Fermi energy in the substrate (all energies here are measured with respect to the band edge deep within the substrate) does not vary as charge in the well is changed. Using terminology defined below, we can write

$$\frac{d(E_{Fw}-E_{Fs})}{dt}=\frac{dU_{\text{bound}}}{dt}+\frac{1}{g_d}\frac{d\sigma_w}{dt}\ . \tag{A1}$$

U_{bound} is the bound-state energy, σ_w is the number density of electronic charge in the well, and g_d is the thermodynamic DOS at the Fermi energy. The inverse of the *thermodynamic* DOS multiplies $d\sigma_w/dt$ in Eq. (A1) because the equilibration of Fermi energies in the quantum well and the substrate occurs on time scales fast compared to the inverse of the measurement frequency. We now define U_w to be the energy of the conduction-band edge in the well at the center of gravity of the ground-state wave function containing the electrons in the 2DEG in the well.

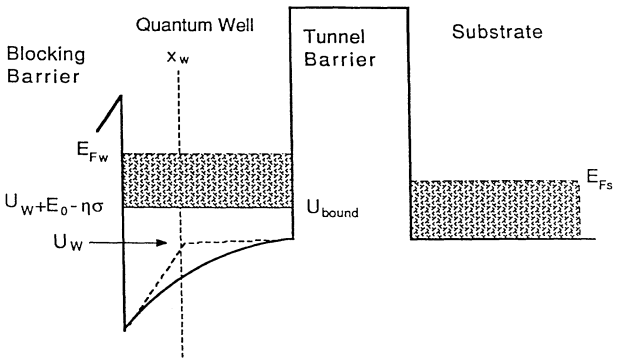

FIG. 13. The figure shows the band diagram of the quantum well, tunnel barrier, and the substrate with the electronic density in the well slightly out of equilibrium with the electronic density in the substrate. The "quasi-Fermi level" in the well E_{Fw} in time relaxes so that it becomes equal to the Fermi energy in the substrate, E_{Fs}; as it changes, U_{bound} also changes.

Elsewhere,[4,5] we have described the term η, which is a correction to the energy of the bound state in the well. The bound-state energy is first considered using a sheet charge model, and its value is taken to be U_w+E_0 where E_0 is a constant energy. Then a correction is made for the finite width of the bound-state wave function so that the bound-state energy is given by

$$U_{\text{bound}}=U_w+E_0-\eta\sigma_w \ .$$

Here, the last term accounts for two effects. One is the difference in the electrostatic energy of the bound state associated with charge being distributed in the well rather than in a sheet. The other is the quantum-mechanical change in the bound-state energy due to the change of the shape of the well bottom in the presence of charge as well as exchange correlation effects.[30] We can then write

$$\frac{dU_{\text{bound}}}{dt}=\frac{dU_w}{dt}-\eta\frac{d\sigma_w}{dt} \ . \tag{A2}$$

The tunneling current may be expressed in terms of a tunneling DOS in the well g_s, at the Fermi energy, and a mean tunneling rate per electron of $1/\tau_{\text{tun}}$:[18]

$$I_{\text{tun}}=Ae(E_{Fw}-E_{Fs})\frac{g_s}{\tau_{\text{tun}}} \ , \tag{A3}$$

where e is the magnitude of the electronic charge and A is the sample area. Note that this expression is correct only for temperatures and applied biases small enough that only electrons in a narrow range over which g_s is constant can tunnel. As was discussed earlier, at higher temperatures, g_s must be replaced with its thermal average. In the "equilibrium tunneling" measurements presented here, $|E_{Fw}-E_{Fs}|$ is always kept less than k_BT by suitable choice of measuring voltage. Given the tunneling current, it is simple to determine $d\sigma_w/dt$ and dU_w/dt. These are given by

$$\frac{d\sigma_w}{dt}=\frac{-I_{\text{tun}}}{Ae}=-(E_{Fw}-E_{Fs})\frac{g_s}{\tau_{\text{tun}}} \tag{A4}$$

and

$$\frac{dU_w}{dt}=\frac{-I_{\text{tun}}}{C_w}=\frac{-Ae}{C_w}(E_{Fw}-E_{Fs})\frac{g_s}{\tau_{\text{tun}}} \ . \tag{A5}$$

Here, C_w is the capacitance, in the sheet charge model, of the quantum well to the surroundings (substrate and top gate). It is given by

$$C_w=C_{\text{geom}}\frac{x_g}{x_g-x_w} \ , \tag{A6}$$

where x_w and x_g are the distances from the substrate charge to the charge in the quantum well and top gate, respectively, and C_{geom} is the "geometric capacitance," $A\epsilon/x_w$, of the quantum-well sheet charge to the substrate.

Rewriting Eq. (A1) again using Eqs. (A2)–(A6) gives

$$\frac{d(E_{Fw}-E_{Fs})}{dt}=-\frac{(E_{Fw}-E_{Fs})}{\tau_{\text{tun}}}\times\left[\frac{Ae^2g_s}{C_{\text{geom}}}\left[1-\frac{x_w}{x_g}\right]-\eta g_s+\frac{g_s}{g_d}\right] .$$

The solution of this first-order differential equation is of course given by an exponential decrease of $E_{Fw}-E_{Fs}$ with time. The relaxation rate is

$$\frac{1}{\tau_r}=\frac{1}{\tau_{\text{tun}}}\left[\frac{Ae^2g_s}{C_{\text{geom}}}\left[1-\frac{x_w}{x_g}\right]-\eta g_s+\frac{g_s}{g_d}\right] . \tag{A7}$$

In our samples, the sum of the first two terms in the square brackets is, in zero magnetic field, of order ten, whereas the third is unity or less. This means that the relaxation rates in our samples are typically faster than the tunneling rates.

This difference between the relaxation rate and the tunneling rate can be explained heuristically as follows. Consider one electron tunneling from or to the quantum well. The transfer of this single electron not only reduces the excess number of electrons on one side of the tunneling barrier but, because of the charge it carries, changes the electrostatic potentials to reduce further the deviation of the system from equilibrium. This "speeds up" the equilibration of the two electron gases. At zero magnetic field in our samples, the average quantum level spacing in the 2D electron gas, $1/Ae^2g_s$, is about 10% of the electrostatic energy for adding one charge to the well, e^2/C_w. This corresponds to about a tenfold increase in the equilibration rate compared to the tunneling rate.

2. Fitting to capacitance and loss tangent curves

Using the expressions above we can calculate the capacitance and the loss tangent for the device as a function of frequency. We start by calculating the current through the device after (at time $t=0$) a voltage δV is suddenly applied between the top gate and the substrate. Only the fraction of $(x_w/x_g)\delta V$ of the applied voltage appears between the well and substrate. Further, only the fraction $(x_w/x_g)I_{\text{tun}}$ of the current which moves between the quantum well and the substrate should be counted in the device current because the current only traverses part way through the device. The total device current is then

$$I_{\text{dev}}(t)=(\delta V)Ae^2\frac{g_s}{\tau_{\text{tun}}}\left[\frac{x_w}{x_g}\right]^2e^{-t/\tau_r}+(\delta V)\frac{C_{\text{high}}}{\tau_{\text{fast}}}e^{-t/\tau_{\text{fast}}} \ . \tag{A8}$$

C_{high} (high-frequency capacitance) is the capacitance of the device with no current traversing the tunnel barrier. In terms of device parameters, its value is $A\epsilon/x_g$. τ_{fast} is the charging time of the capacitance C_{high} due to any resistance in series with our device. We consider τ_{fast} to be much shorter than the period of the measuring signals in our experiment.

The ac admittance of the device is given by $j\omega$ times the Fourier transform of this "step response." In the lim-

it where τ_{fast} goes to zero, the ac current through the sample is

$$I = Ae^2 \frac{g_s}{\tau_{\text{tun}}} \left[\frac{x_w}{x_g} \right]^2 \frac{\omega^2\tau_r^2 + j\omega\tau_r}{1+\omega^2\tau_r^2} V + j\omega C_{\text{high}} V \ , \qquad \text{(A9)}$$

where V is the amplitude of the measuring voltage $Ve^{j\omega t}$. The tunneling conductance is given by

$$G_{\text{tun}} = Ae^2 \frac{g_s}{\tau_{\text{tun}}} \ . \qquad \text{(A10)}$$

Rewriting Eq. (A9) again, dividing by the voltage, we find that the device admittance is

$$Y(\omega) = G_{\text{tun}} \left[\frac{x_w}{x_g} \right]^2 \frac{\omega^2\tau_r^2}{1+\omega^2\tau_r^2} + j\omega \left[G_{\text{tun}} \left[\frac{x_w}{x_g} \right]^2 \frac{\tau_r}{1+\omega^2\tau_r^2} + C_{\text{high}} \right] . \qquad \text{(A11)}$$

The term in the square brackets of this equation can immediately be identified as the device capacitance. The loss tangent for the sample is given by the real part of the admittance divided by the imaginary part.

We can now write down the device capacitance and loss tangent as functions of frequency. From Eq. (A11) for the sample admittance above, we find for the capacitance

$$C(f) = \frac{C_{\text{high}} C_{\text{low}} [1 + (f/f_{\text{peak}})^2]}{C_{\text{high}} + C_{\text{low}} (f/f_{\text{peak}})^2} \ , \qquad (1)$$

and for the loss tangent

$$D(f) = 2d_{\text{peak}} \frac{f/f_{\text{peak}}}{1+(f/f_{\text{peak}})^2} \ . \qquad \text{(A12)}$$

Here, the loss tangent peak height D_{peak} is given by

$$D_{\text{peak}} = \left[\frac{C_{\text{high}}}{C_{\text{low}}} \right]^{1/2} \left[\frac{C_{\text{low}}}{C_{\text{high}}} - 1 \right] , \qquad \text{(A13)}$$

and the frequency at which the loss tangent goes through a peak f_{peak} is related to the tunneling conductance in the following fashion:

$$G_{\text{tun}} = 2\pi f_{\text{peak}} C_{\text{geom}} \frac{C_{\text{geom}}}{\sqrt{C_{\text{low}} C_{\text{high}}}} \left[\frac{C_{\text{low}}}{C_{\text{high}}} - 1 \right] . \qquad (2)$$

Note that to arrive at Eq. (2) we have made substantial use of the formulas relating g_d and η to C_{low}, C_{high}, and C_{geom} described elsewhere.[5] The value of C_{geom} used here is known to within 2% using the methods described in Ref. 4. Note that in the presence of low in-plane conductivity of the 2D electron gas, Eqs. (1) and (A12) must be modified somewhat in order to properly fit the data.[5] The fits given by Eqs. (1) and (A12) are identical to the functional forms for the capacitance and the loss tangent indicated by the circuit model of Fig. 1(b), but the interpretation of the fitting parameters is different.

*Present address: Department of Physics, Massachussetts Institute of Technology, Cambridge, MA 02139.
†Present address: Eastman Kodak Co., Rochester, NY 14650.
‡Present address: Department of Physics and Astronomy, University of Rochester, Rochester, NY 14627.

[1]R. C. Ashoori, J. A. Lebens, N. P. Bigelow, and R. H. Silsbee, Phys. Rev. Lett. **64**, 681 (1990).
[2]J. Smoliner, W. Demmerle, G. Berthold, E. Gornik, G. Weimann, and W. Schlapp, Phys. Rev. Lett. **63**, 2116 (1989).
[3]J. P. Eisenstein, T. J. Gramila, L. N. Pfeiffer, and K. W. West, Phys. Rev. B **44**, 6511 (1992).
[4]R. C. Ashoori and R. H. Silsbee, Solid State Commun. **81**, 821 (1992).
[5]R. C. Ashoori,Ph.D. thesis, Cornell University, 1991.
[6]T. P. Smith, B. B. Goldberg, P. J. Stiles, and M. Heiblum, Phys. Rev. B **32**, 2696 (1985).
[7]E. Böckenhoff, K. v. Klitzing, and K. Ploog, Phys. Rev. B **38**, 10 120 (1988).
[8]B. R. Snell, K. S. Chan, F. W. Sheard, L. Eaves, G. A. Toombs, D. K. Maude, J. C. Portal, S. J. Bass, P. Claxton, G. Hill, and M. A. Pate, Phys. Rev. Lett. **59**, 2806 (1987).
[9]J. A. Lebens, R. H. Silsbee, and S. L. Wright, Appl. Phys. Lett. **51**, 840 (1987).
[10]J. A. Lebens, R. H. Silsbee, and S. L. Wright, Phys. Rev. B **37**, 10 308 (1988).
[11]J. A. Lebens, Ph.D. thesis, Cornell University, 1988.
[12]E. Gornik, R. Lussnig, G. Strasser, H. L. Störmer, A. C. Gossard, and W. Wiegmann, Phys. Rev. Lett. **54**, 1820 (1985).
[13]S. Das Sarma and Frank Stern, Phys. Rev. B **32**, 8442 (1985).
[14]A. L. Efros, in *Proceedings of the Twentieth International Conference on the Physics of Semiconductors,* edited by E. M. Anastassakis and J. D. Joannopoulos (World Scientific, Singapore, 1990).
[15]A. L. Efros, Phys. Rev. B **45**, 11 354 (1990).
[16]P. A. Lee, Phys. Rev. B **26**, 5882 (1982).
[17]T. W. Hickmott, Phys. Rev. Lett. **57**, 751 (1986).
[18]E. L. Wolf, *Principles of Electron Tunneling Spectroscopy* (Oxford University Press, New York, 1985), Chap. 2.
[19]John A. Nixon and John H. Davies, Phys. Rev. B **41**, 7929 (1990).
[20]S. J. Allen, Jr., D. C. Tsui, and F. DeRosa, Phys. Rev. Lett. **35**, 1359 (1975).
[21]A. Gold, S. J. Allen, B. A. Wilson, and D. C. Tsui, Phys. Rev. B **25**, 3519 (1982).
[22]D. J. Bishop, D. C. Tsui, and R. C. Dynes, Phys. Rev. Lett. **44**, 1153 (1980).
[23]B. L. Altshuler, A. G. Aronov, and P. A. Lee, Phys. Rev. Lett. **44**, 1288 (1980).
[24]Yoseph Imry and Zvi Ovadyahu, Phys. Rev. Lett. **49**, 841 (1982).
[25]Alice E. White, R. C. Dynes, and J. P. Garno, Phys. Rev. B **31**, 1174 (1985).
[26]A. L. Efros and B. I. Shklovskii, J. Phys. C **8**, L49 (1975).
[27]H. W. Jiang, R. L. Willett, H. L. Störmer, D. C. Tsui, L. N. Pfeiffer, and K. W. West, Phys. Rev. Lett. **65**, 633 (1990).
[28]J. P. Eisenstien, L. N. Pfeiffer, and K. W. West, Phys. Rev. Lett. **69**, 3804 (1992).
[29]Kazuhiko Hirakawa and Hiroyuki Sakaki, Phys. Rev. B **33**, 8291 (1986).
[30]A. L. Efros, Solid State Commun. **65**, 1281 (1988).